

## DETERMINATION OF GAS MIXTURE COMPONENTS USING FLUCTUATION ENHANCED SENSING AND THE LS-SVM REGRESSION ALGORITHM

**Łukasz Lentka<sup>1)</sup>, Janusz M. Smulko<sup>1)</sup>, Radu Ionescu<sup>2)</sup>, Claes G. Granqvist<sup>3)</sup>,  
Laszlo B. Kish<sup>4)</sup>**

1) Gdańsk University of Technology, Faculty of Electronics, Telecommunications and Informatics, G. Narutowicza 11/12, 80-233 Gdańsk, Poland (lukasz.lentka@gmail.com, ✉ jsmulko@eti.pg.gda.pl +48 58 348 6095)

2) Rovira i Virgili University, ETSE-DEEEA, Department of Electronics, Carrer de l'Escorçador, 43003 Tarragona, Spain (radu.ionescu@urv.cat)

3) Uppsala University, Department of Engineering Sciences, P.O. Box 534, SE-75121 Uppsala, Sweden (Claes-Goran.Granqvist@Angstrom.uu.se)

4) Texas A&M University, Department of Electrical and Computer Engineering, College Station, TX 77843-3128, USA (Laszlo.Kish@ece.tamu.edu)

### Abstract

This paper analyses the effectiveness of determining gas concentrations by using a prototype WO<sub>3</sub> resistive gas sensor together with fluctuation enhanced sensing. We have earlier demonstrated that this method can determine the composition of a gas mixture by using only a single sensor. In the present study, we apply Least-Squares Support-Vector-Machine-based (LS-SVM-based) nonlinear regression to determine the gas concentration of each constituent in a mixture. We confirmed that the accuracy of the estimated gas concentration could be significantly improved by applying temperature change and ultraviolet irradiation of the WO<sub>3</sub> layer. Fluctuation-enhanced sensing allowed us to predict the concentration of both component gases.

Keywords: LS-SVM algorithm, resistance gas sensor, fluctuation enhanced sensing, gas detection.

© 2015 Polish Academy of Sciences. All rights reserved

### 1. Introduction

Awareness of concentration, or even presence, of hazardous gases is crucial for protecting life and health of human beings in numerous cases [1–6]. In real-world applications we deal with a mixture of various gases and have to develop detection methods that are robust to the presence of background gases or humidity. Resistive gas sensors detect various gases by recording mainly their DC resistance changes. Therefore a gas mixture can be determined by applying a matrix of gas sensors with varying sensitivity to different gases. However, such a solution tends to be expensive and is highly energy-consuming. Smarter solutions use a limited number of sensors, but require more advanced measurements, like DC changes of the gas sensor when its temperature is modulated or fluctuation enhanced sensing utilizing resistance fluctuations [3]. An algorithm is then needed to determine concentrations of the detected gases.

In this experimental study, a prototype WO<sub>3</sub> gas sensing layer was used to investigate the efficiency of a detection algorithm for determining the gas concentration of a selected gas mixture. The gas sensing layer was prepared as reported elsewhere [7]. The investigated WO<sub>3</sub> layer changes its gas sensing properties when modulated by temperature changes or ultraviolet (UV) irradiation. We propose to utilize both factors to modulate the sensor's physical properties in order to ultimately improve the efficiency for gas detection. The power spectral density of voltage noise  $S_u(f)$  across the gas sensor, driven by a constant current in the negative feedback of an operational amplifier, was measured. The applied algorithm used a data vector of the spectrum  $S_u(f)$  normalized by the squared DC bias voltage  $U$ . These data are independent of

the measurement setup and result from resistance fluctuations when the sensor bias voltage is above at least a few hundred mV to reduce the influence of the inherent noise of the operational amplifier.

The normalized power spectral density  $S_u(f)/U^2$  was used as input data vector for the detection algorithm. This input vector was extended by adding the same product  $S_u(f)/U^2$ , but observed at various conditions. This strategy helped us to elucidate how the methods improved the efficiency for gas detection.

We used exemplary gas mixtures of NO<sub>2</sub> and ethanol (C<sub>2</sub>H<sub>5</sub>OH) of various concentrations. The sensor response to changes of the ambient atmosphere (gas concentration) is usually nonlinear, and therefore we decided to apply a nonlinear algorithm, which should assure better detection under conditions of nonlinearity. We proposed to apply the Support Vector Machine (SVM) algorithm as in other similar cases, such as for electro-catalytic gas sensors [6] or in Raman spectroscopy [8], where the input data form a vector of partially correlated values. The correlation is unknown and can change for data observed at various gas compositions. Therefore we have to apply an algorithm which can be efficient in different situations.

The SVM algorithm is a supervised machine-learning method, which can operate in one of two modes: classification or function estimation (regression). Here we used the least squares version of the SVM (called LS-SVM) in the regression mode to determine concentrations of gas mixture constituents. The applied algorithm can perform the necessary computations faster than its previous versions.

The SVM method was earlier [9] applied to fluctuation-enhanced sensing in order to detect the presence of a large set of various agents in gas mixtures. In the present paper we go further by achieving a *quantitative* analysis of the given agent in a gas mixture by enriching the measurement information through selection of working point conditions.

## 2. Measurement system and data pre-processing

Figure 1 presents a block diagram of the measurement system. The resistive gas sensor was placed in a chamber of 1 litre volume, and the gas flow was controlled by three independent flow-meters to supply a mixture of two gases: NO<sub>2</sub> together with ethanol diluted in synthetic air. The combined continuous output gas flow did not exceed 100–200 ml/min; this avoided turbulence which might otherwise have influenced the observed noise. These conditions assured that the recorded noise was stationary (Fig. 2). Other details of the measurement setup can be found elsewhere [7].

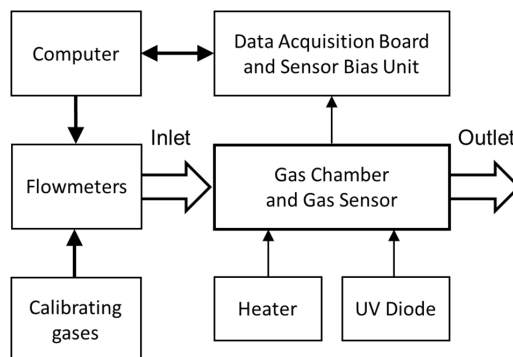


Fig. 1. Block diagram of the measurement setup.

The properties of the gas sensor were modulated by changing their working temperature or by using UV irradiation. Both factors influenced the sensitivity and selectivity of the WO<sub>3</sub> sensor film, which is consistent with other findings for various gas sensing layers [1, 5, 7]. The influence of temperature changes or of UV irradiation can be different for the investigated gas sensing layers and gas mixtures. Therefore we were not able to ascertain which of the methods would be more efficient for determining gas concentration prior to performing the computations. The observed low-frequency noise depended on the applied working conditions, and 1/*f*-like noise dominated in different frequency ranges. We decided to estimate power spectral densities up to a few kHz only when the 1/*f* noise component prevailed. The sampling frequency was set to  $f_s = 4$  kHz. Normalized power spectral densities were estimated by using voltage noise records observed during 500 s and comprising about  $2 \times 10^6$  samples in order to reduce the random error by averaging over the set of estimated spectra. The power spectral densities were then employed as input data for the LS-SVM algorithm.

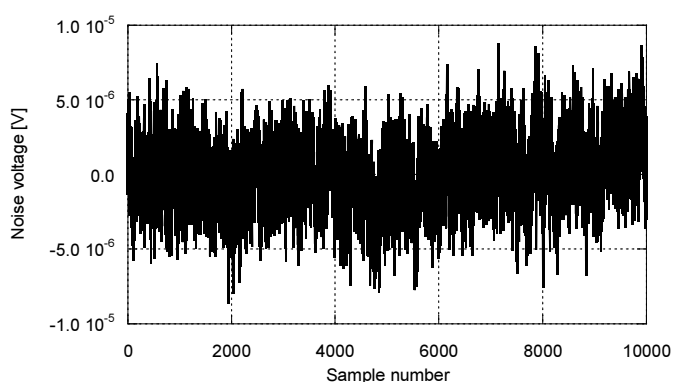


Fig. 2. Exemplary time record of observed voltage noise.

We considered four different concentrations (0, 10, 20, and 50 ppm) of NO<sub>2</sub> as well as the same concentrations of C<sub>2</sub>H<sub>5</sub>OH diluted in synthetic air. Thus we obtained sixteen different combinations altogether. The case when both gas concentrations were equal to zero corresponds to flow of synthetic air only. The measurements were done at two sensor temperatures: 100 and 225°C, and at two UV diode currents: 0 (without UV irradiation) and 6 mA in which case the effect of UV irradiation on the gas sensing layer was saturated (the same results were observed with higher currents applied to the UV diode). In this way we obtained four combinations of measurement conditions, given in Table 1.

Table 1. Measurement conditions for recording resistance noise.

UV LED current [mA]	Temperature [°C]
0 (UV diode off)	100
	225
6 (UV diode on)	100
	225

The noise records (each consisting of  $2 \times 10^6$  samples) were taken to represent 50 independent spectra for each set of measurement conditions (Table 1) for all 16 combinations of concentrations of two gases, thus giving a total of  $50 \times 4 \times 16 = 3200$  spectra. Each spectrum was estimated from a record of 40 960 voltage noise samples by computing spectra from consecutive time records, each 1024 noise samples long, and averaging 40 of them to reduce

the random error of the estimated power spectra to as little as 16%. The latter value represents a compromise between accuracy of noise measurement and time for noise recording to collect a sufficient number of samples.

The estimated set of 50 spectra for each combination of measurement conditions and gas concentrations was divided into two subsets. A set of 40 spectra was used to establish a mathematical model for the LS-SVM algorithm, and the remaining 10 spectra were employed to test the accuracy of the model. Each of these 50 spectra has a length of 513 points including the DC component. Only a part of these frequency bins could be used for gas detection. At frequencies close to the maximum frequency of the spectrum (for  $f_s/2$ ) the values were attenuated by an antialiasing filter. At very low frequencies, typically covering the first 2–3 frequency bins, the estimated spectra values exhibited a high variance due to unavoidable drifts. Therefore we decided to limit the estimated values by rejecting the first three and last 22 bins of each spectrum and eventually obtained  $513 - 3 - 22 = 488$  frequency bins.

Four cases of input data-shown in Table 2 – were considered. The length of the input data started from 488 points in the first case and reached  $4 \times 488 = 1952$  points in the last one, when all measurement conditions were used to predict gas concentration. The aim of constructing such data sets was to identify which of the working conditions for the gas sensing layer were more informative and gives better accuracy for predicting gas concentrations.

Table 2. Input data vectors for the LS-SVM algorithm.

No.	Measurement conditions	Data length
1	{100 °C, 0 mA}	488
2	{100 °C, 0 mA} and {100 °C, 6 mA}	976
3	{100 °C, 0 mA} and {100 °C, 6 mA} and {225 °C, 0 mA}	1464
4	{100 °C, 0 mA} and {100 °C, 6 mA} and {225 °C, 0 mA} and {225 °C, 6 mA}	1952

### 3. SVM algorithm

The SVM algorithm is one of the popular techniques of supervised machine learning; it was proposed by Vapnik [10]. The fundamentals of this method, and various applications for predicting chemical compound concentration, have been presented elsewhere [6, 8, 11–15]. The algorithm attracted huge interest among scientists because it is based on a very simple idea and leads to high performance in numerous practical applications [14, 16–18]. The algorithm was developed originally for pattern recognition by learning from exemplary data belonging to two opposite sets. The classification is based on the class of hyper-planes, defined in multi-dimensional space by a vector  $w$  orthogonal to that hyper-plane and maximizing the difference between these classes.

A regression algorithm was developed for situations wherein the data are divided not into two separate classes but can predict values of a continuous function. The LS-SVM algorithm is its-least squares version and was proposed by Suykens [11]. The latter algorithm transforms a quadratic programming problem into a linear problem and makes the necessary computations much faster. The Matlab toolbox, used freely for research, provides all necessary and basic functions of this method [15]. Our study used the LS-SVMLab toolbox v1.8. The LS-SVM algorithm finds an optimal solution by solving a system of linear equations, which is rather a trivial computing task for today's computers. The algorithm can operate in either of two modes: classification mode or regression mode (for function estimation). The regression mode can predict function values by using the mathematical model created at the entry stage. This task can be performed by the LS-SVM algorithm in our experimental studies to predict

concentrations of mixed gases and determine which of the working conditions for the gas sensing layer is more informative.

### 3.1. The LS-SVM regression algorithm

In the least-squares version of the SVM algorithm, the original problem of determining solutions to predict function values (*e.g.*, gas concentrations) is modified at two points. Firstly, the inequality constraints of the minimization problem with a slack variable are replaced by equality constraints with an error  $e_k$ . Secondly, a squared loss function is considered as the objective function to determine the learning model necessary for predicting gas concentrations. After applying these two modifications, the problem becomes a linear problem which is simple to solve.

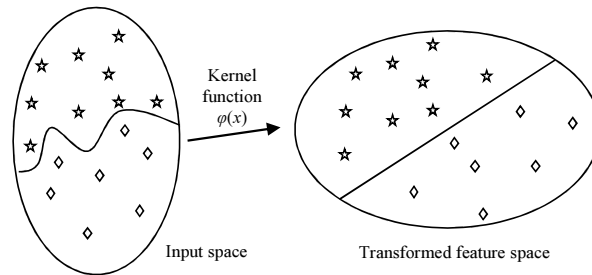


Fig. 3. Illustration of using a nonlinear kernel function  $\phi(x)$  in the SVM algorithm.

The fundamentals of the LS-SVM algorithm are presented below, following [11] and [14]. Let us consider a given training dataset  $\{x_k, y_k\}_{k=1}^N$  with  $x_k \in \mathfrak{R}^n$  and  $y_k \in \mathfrak{R}$ . The nonlinear LS-SVM method uses nonlinear mapping, represented by the kernel function  $\phi(x)$  (Fig. 3), to deal with a nonlinear dataset. Then we can present the LS-SVM model as a feature space representation of the data set, given by the equation:

$$y(x) = w^T \phi(x) + b. \tag{1}$$

To find the optimal value of  $w$  and  $b$ , we have to solve the optimization problem, which means maximizing the margin  $1/\|w\|$  and minimizing the learning error:

$$\min_{w, e} J(w, e) = \frac{1}{2} w^T w + \gamma \frac{1}{2} \sum_{k=1}^N e_k^2, \tag{2}$$

which is subject to equality constraints according to:

$$y_k = w^T \phi(x_k) + b + e_k, \quad k = 1, \dots, N. \tag{3}$$

The Lagrangian function of the above equation is:

$$L(w, b, e, \alpha) = J(w, e) - \sum_{k=1}^N \alpha_k \{w^T \phi(x_k) + b + e_k - y_k\}, \tag{4}$$

where  $\alpha_k$  are Lagrangian multipliers. The optimal point of the Lagrangian function is in its saddle point, determined by the following conditions:

$$\left\{ \begin{array}{l} \frac{\partial L}{\partial w} = 0 \rightarrow w = \sum_{k=1}^N \alpha_k \phi(x_k) \\ \frac{\partial L}{\partial b} = 0 \rightarrow \sum_{k=1}^N \alpha_k = 0 \\ \frac{\partial L}{\partial e_k} = 0 \rightarrow \alpha_k = \gamma e_k, \quad k = 1, \dots, N \\ \frac{\partial L}{\partial \alpha_k} = 0 \rightarrow w^T \phi(x_k) + b + e_k - y_k = 0, \quad k = 1, \dots, N. \end{array} \right. \quad (5)$$

We can see that the system (5), obtained from the Karush-Kuhn-Tucker conditions [19], is linear. A solution of such equations can be found by solving a system of linear equations using standard methods such as conjugate gradient descent.

The system of linear equations can be presented in matrix form by:

$$\begin{bmatrix} 0 & \bar{1}^T \\ \bar{1} & \Omega + \gamma^{-1}I \end{bmatrix} \begin{bmatrix} b \\ \alpha \end{bmatrix} = \begin{bmatrix} 0 \\ y \end{bmatrix}, \quad (6)$$

where:  $y = [y_1; \dots; y_N]$ ,  $\bar{1} = [1; \dots; 1]$ ,  $\alpha = [\alpha_1; \dots; \alpha_N]$ , and – after applying Mercer’s condition [20] –  $\Omega_{kl} = \varphi(x_k)^T \varphi(x_l) = K(x_k, x_l)$ ,  $k, l = 1, \dots, N$ . A radial basis kernel function (RBF) can be used in order to model a nonlinear process. For our purposes, this function is  $\Omega_{kl} = \exp\left(-\|x_k^T - x_l^T\|^2 / \sigma^2\right)$ . Finally the resulting LS-SVM model is:

$$y(x) = \sum_{k=1}^N \alpha_k K(x_k, x) + b. \quad (7)$$

SVM implementation requires three tuning parameters ( $\gamma, \sigma, \varepsilon$ ), while LS-SVM requires only two tuning parameters ( $\gamma, \sigma$ ). A disadvantage of both methods is that the training time increases with the square of the number of training samples ( $N$ ) and linearly with the number of variables (dimension of the investigated spectra), which is opposite to the case of classic least-squares methods using principal component analysis algorithm [16].

### 3.2. Application of the LS-SVM algorithm

In earlier work [8], the authors showed that LS-SVM gives more accurate results and is substantially more robust to additive noise than conventional regression methods which apply linear functions only (e.g., the Principal Component Analysis method [21]). The LS-SVM method also provides a high degree of accuracy for concentration prediction, particularly for data sets for which a considerable nonlinearity can be expected. We know that the response of the gas sensors – i.e., the change of their DC resistance or resistance noise power spectrum – to changes of the ambient atmosphere is nonlinear. An analogous nonlinear relation occurs when the ambient atmosphere consists of a gas mixture of various proportions. Thus the LS-SVM algorithm is expected to be very efficient for gas concentration prediction. This property ensues because the kernel function provides nonlinear conversion of the input feature space into the higher-dimensional transformed input space where the data are linearly separable.

The most popular kernel functions are polynomial, sigmoidal or Gaussian RBFs. Here we used the latter because the main error of the recorded data is the random error of the estimated power spectral densities due to limited averaging time. The RBF kernel function should work

well with such a source of data inaccuracy, as considered also in other regression problems [8, 16].

There are many papers discussing the use of the SVM method for data processing in gas sensing [6, 12, 16–18]. We should emphasize the necessity of careful selection of LS-SVM model parameters to obtain high accuracy of gas concentration prediction. It is important to select optimal values of these parameters in order to get the most reliable results of gas concentration prediction, as discussed for similar cases [22, 23]. In our experimental study, these parameters were selected by applying the function *tunelssvm* available in the Matlab toolbox [15]. This function determines the optimal value of the RBF kernel parameter  $\sigma^2$  and the regularization parameter  $\gamma$  at the stage of learning (model creation). The function *tunelssvm* uses different optimization algorithms. First, good starting points are found by rough approximation and then the final adjustment is reached by the *simplex* method.

#### 4. Results of gas concentration prediction

Figures 4 and 5 present results of gas concentration prediction using the LS-SVM regression algorithm for a set of 160 test data vectors for the cases #1 and #4, respectively (Table 2). We can see that longer input data vectors assure better accuracy of the regression algorithm, *i.e.*, lower values of the root mean square error  $\sigma_e$  of gas concentration prediction (Fig. 6). Such results are obvious, because a longer input vector is more informative and should assure more appropriate regression, as predicted in theoretical considerations for nonlinear methods [8]. On the other hand, we can see that the worst results of gas concentration prediction are found when  $C_2H_5OH$  and  $NO_2$  have similar concentrations in the mixture (*e.g.*, results in Fig. 5 when both gases have a concentration of  $\sim 20$  ppm). The highest accuracy of gas concentration prediction took place when one of the gases dominated in the investigated gas mixture (*i.e.*, when their concentrations were strongly different, as when only one gas was present in the mixture; Fig. 4).

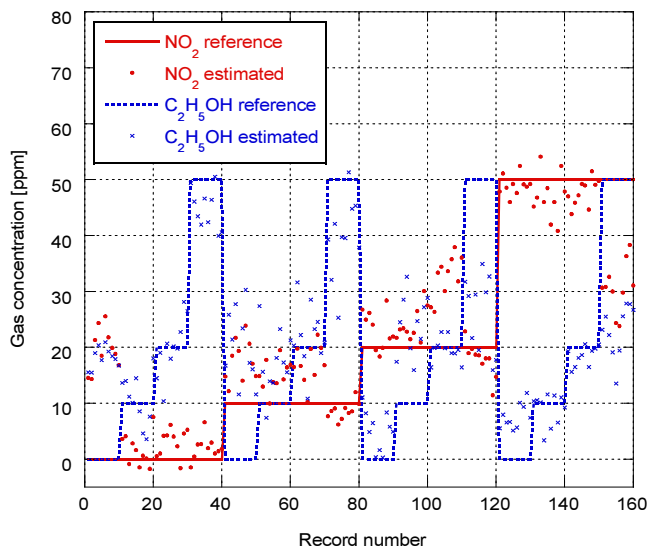


Fig. 4. Results of the regression algorithm obtained for the case #1, presented in Table 2.

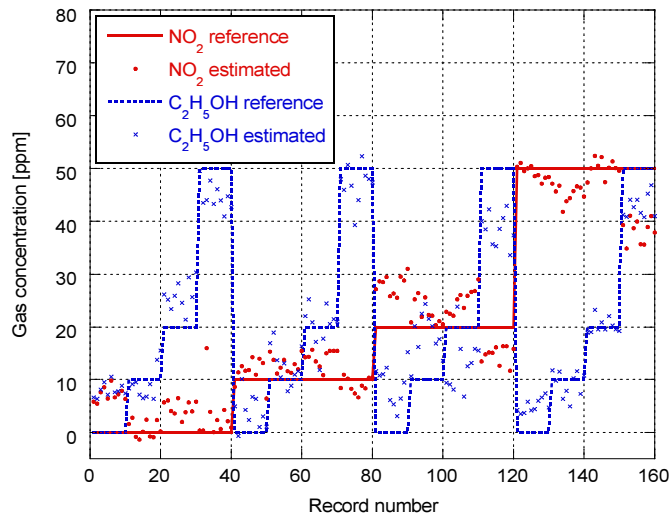


Fig. 5. Results of the regression algorithm obtained for the case #4, presented in Table 2.

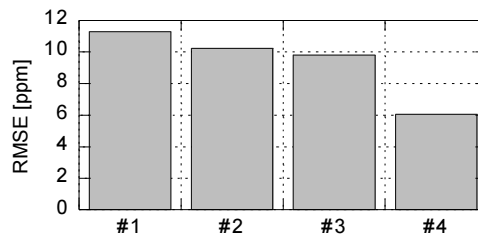


Fig. 6. Root mean square error RMSE of gas concentration prediction using the LS-SVM regression algorithm for the measurement data sets in Table 2.

We can observe a significant decrease of the root mean square error in the case #4. In other cases, the error is so large that the concentration prediction error is too high to be accepted for hazardous gases. Despite its inconveniences – a more complex calculation and longer time of model generation – case #4 is most reliable and should be chosen for practical applications.

We should mention that the measurement conditions give different information and should be selected very carefully to assure the best gas detection results. Thus additional calculations to create a regression model were performed when the input data were only 488 frequency bins long (as in case #1, Table 2) but representing different working conditions (the temperature of the gas sensing layer, and the current for the UV diode irradiating the layer) of the gas sensor, specifically (a) 100°C, 6 mA; (b) 225°C, 0 mA; and (c) 225°C, 6 mA. We calculated the root mean square error RMSE of gas concentration prediction separately for the above mentioned conditions and obtained the following results: (a) RMSE = 11.7 ppm, (b) RMSE = 10.9 ppm, and (c) RMSE = 7.9 ppm. This means that the most informative noise data for detecting the considered gas mixture (NO<sub>2</sub> and C<sub>2</sub>H<sub>5</sub>OH) were collected at the conditions 225 °C, 6 mA. We were able to conclude that these conditions assured an error of gas concentration prediction that was ~40% lower than for other considered conditions.

The presented procedure and the use of the LS-SVM algorithm helped to determine which of the working conditions, applied to the investigated gas sensing layer, was most informative for gas detection. The goal was to achieve a quantitative gas composition analysis (an important



aspect of metrology [24]) by utilizing fluctuation-enhanced sensing. We should underscore that the method does not require any additional data processing (*e.g.*, background noise removal, spectra smoothing, *etc.*), which is common in other chemo-metric methods [25]. This is a benefit of the LS-SVM method, because any additional pre-processing method demands optimal selection of some additional parameters before its use. We should also emphasize that the presented results do not consider a dependence of gas concentration prediction on accuracy of the estimated noise spectra. This problem is still open, especially when we have to consider some unavoidable drifts at the very low frequency range [26] and their influence on the LS-SVM method [8].

## 5. Conclusions

This experimental study presented a method for predicting the concentration of gases by using a single gas sensor. We proved that the LS-SVM method can predict the concentration of gas mixture components (NO<sub>2</sub> and ethanol) by applying fluctuation enhanced sensing. The LS-SVM method helped us to establish the working conditions of the investigated gas sensing layer for which the prediction of gas concentrations was the most accurate, exceeding results obtained under other measurement conditions by 40%. We are confident that the procedure delineated in the present work can be applied successfully for a variety of gases and for different sensing layers.

## Acknowledgements

We would like to thank Maciej Trawka, PhD student, for providing detailed noise records. This work was supported by the National Science Center, Poland, Grant Agreement DEC-2012/06/M/ST7/00444 “Detection of gases by means of nano-technological resistance sensors”. C. G. Granqvist was supported from the European Research Council under the European Community’s Seventh Framework Program (FP7/2007–2013)/ERC Grant Agreement No. 267234 “GRINDOOR”. R. Ionescu acknowledges support from the ‘Ramón y Cajal’ fellowship awarded by the Spanish Ministry for Science and Competiveness (MINECO).

## References

- [1] Zakrzewska, K. (2001). Mixed oxides as gas sensors. *Thin Solid Films*, 391, 229–238.
- [2] Osowski, S., Siwek, K., Grzywacz, T., Brudzewski, K. (2014). Differential electronic nose in on-line dynamic measurements. *Metrol. Meas. Syst.*, 21(4), 649–662.
- [3] Kish, L.B., Vajtai, R., Granqvist, C.G. (2000). Extracting information from noise spectra of chemical sensors: single sensor electronic noses and tongues. *Sensors and Actuators B: Chemical*, 71(1), 55–59.
- [4] Kotarski, M., Smulko, J. (2009). Noise measurement set-ups for fluctuations-enhanced gas sensing. *Metrol. Meas. Syst.*, 16(3), 457–464.
- [5] Korotcenkov, G., Cho, B.K. (2013). Engineering approaches for the improvement of conductometric gas sensor parameters. Part 1. Improvement of sensor sensitivity and selectivity (short survey). *Sensors and Actuators B: Chemical*, 188, 709–728.
- [6] Kalinowski, P., Woźniak, L., Strzelczyk, A., Jasinski, P., Jasinski, G. (2013). Efficiency of linear and non-linear classifiers for gas identification from electrocatalytic gas sensor. *Metrol. Meas. Syst.*, 20(3), 501–512.
- [7] Trawka, M., Smulko, J., Hasse, L., Ionescu, R., Annanouch, F.E., Llobet, E., Granqvist, C.G., Kish, L.B. (2014). Fluctuation enhanced gas sensing using UV irradiated Au-nanoparticle-decorated WO<sub>3</sub>-nanowire films. *Proc. of the 8th International Conference on Sensing Technology*, Sept. 2–4, 2014, Liverpool, UK, 282–286.

- [8] Barman, I., Dingari, N.C., Singh, G.P., Soares, J.S., Dasari, R.R., Smulko, J.M. (2012). Investigation of noise-induced instabilities in quantitative biological spectroscopy and its implications for noninvasive glucose monitoring. *Analytical Chemistry*, 84(19), 8149–8156.
- [9] Ayhan, B., Kwan, C., Zhou, J., Kish, L.B., Benkstein, K.D., Rogers, P.H., Semancik, S. (2013). Fluctuation enhanced sensing (FES) with a nanostructured, semiconducting metal oxide film for gas detection and classification. *Sensors and Actuators B: Chemical*, 188, 651–660.
- [10] Vapnik, V. (2000). *The nature of statistical learning theory*. New York: Springer Science & Business Media.
- [11] Van Gestel, T., De Brabanter, J., De Moor, B., Vandewalle, J., Suykens, J.A.K., Van Gestel, T. (2002). *Least squares support vector machines*, 4, Singapore, World Scientific.
- [12] Pardo, M., Sberveglieri, G. (2005). Classification of electronic nose data with support vector machines. *Sensors and Actuators B: Chemical*, 107(2), 730–737.
- [13] Kwiatkowski, A., Czerwicka, M., Smulko, J., Stepnowski, P. (2014). Detection of denatonium benzoate (Bitrex) remnants in noncommercial alcoholic beverages by raman spectroscopy. *Journal of Forensic Sciences*, 59(5), 1358–1363.
- [14] Adankon, M.M., Cheriet, M. (2009). Model selection for the LS-SVM. Application to handwriting recognition. *Pattern Recognition*, 42(12), 3264–3270.
- [15] Pelckmans, K., Suykens, J.A., Van Gestel, T., De Brabanter, J., Lukas, L., Hamers, B., De Moor, B. (2002). *LS-SVMlab: a matlab/c toolbox for least squares support vector machines*.
- [16] Chauchard, F., Cogdill, R., Roussel, S., Roger, J. M., Bellon-Maurel, V. (2004). Application of LS-SVM to non-linear phenomena in NIR spectroscopy: development of a robust and portable sensor for acidity prediction in grapes. *Chemometrics and Intelligent Laboratory Systems*, 71(2), 141–150.
- [17] Kaur, R., Kumar, R., Gulati, A., Ghanshyam, C., Kapur, P., Bhondekar, A.P. (2012). Enhancing electronic nose performance: A novel feature selection approach using dynamic social impact theory and moving window time slicing for classification of Kangra orthodox black tea (*Camellia Sinensis* (L.) O. Kuntze). *Sensors and Actuators B: Chemical*, 166, 309–319.
- [18] Kumar, R., Bhondekar, A.P., Kaur, R., Vig, S., Sharma, A., Kapur, P. (2012). A simple electronic tongue. *Sensors and Actuators B: Chemical*, 171, 1046–1053.
- [19] Kuhn, H.W.; Tucker, A.W. (1951). Nonlinear programming. *Proc. of the 2nd Berkeley Symposium*. Berkeley, University of California Press, 1951, 481–492.
- [20] Hazewinkel, M. (2001). *Mercer theorem*. *Encyclopedia of Mathematics*. Springer.
- [21] Jolliffe, I. (2002). *Principal component analysis*. London: John Wiley & Sons, Ltd.
- [22] Nguyen, M.H., De la Torre, F. (2010). Optimal feature selection for support vector machines. *Pattern Recognition*, 43(3), 584–591.
- [23] Aydin, I., Karakose, M., Akin, E. (2011). A multi-objective artificial immune algorithm for parameter optimization in support vector machine. *Applied Soft Computing*, 11(1), 120–129.
- [24] Mroczka, J. (2013). The cognitive process in metrology. *Measurement*, 46(8), 2896–2907.
- [25] Kwiatkowski, A., Gnyba, M., Smulko, J., Wierzba, P. (2010). Algorithms of chemicals detection using raman spectra. *Metrol. Meas. Syst.*, 17(4), 549–559.
- [26] Granqvist, C.G., Green, S., Jonson, E.K., Marsal, R., Niklasson, G.A., Roos, A., Kish, L.B. (2008). Electrochromic foil-based devices: Optical transmittance and modulation range, effect of ultraviolet irradiation, and quality assessment by  $1/f$  current noise. *Thin Solid Films*, 516(17), 5921–5926.